Received 31 October 2023
Revised 28 February 2024
Accepted 9 May 2024

Improved compensation networks for dynamic wireless power transfer in a multi-inductor track

Manuele Bertoluzzo
Department of Industrial Engineering, University of Padova, Padova, Italy

Paolo Di Barba
Department of Electrical, Computer and Biomedical Engineering, University of Pavia, Pavia, Italy

Michele Forzan
Department of Industrial Engineering, University of Padua, Padua, Italy

Maria Evelina Mognaschi
Department of Electrical, Computer and Biomedical Engineering, University of Pavia, Pavia, Italy, and

Elisabetta Sieni
DISTA, University of Insubria, Varese, Italy

Abstract

Purpose – The purpose of the study is to design the compensation network of a dynamic wireless power transfer system, considering the movement of the receiving coil along an electrified track with a large number of inductors buried on the road.

Design/methodology/approach – A finite element model has been developed to calculate the self-inductances of transmitting and receiving coils as well as the mutual inductances between the receiving coil and the transmitting ones in the nearby and for various relative positions. The calculated lumped parameters, self-inductances and mutual inductances depending on the relative positions between the coils, have been considered to design the compensation network of the active coils, which is composed of three capacitive or inductive reactances connected in the T form. The optimal values of the six reactances, three for the transmitting coils and three for the receiving one, have been calculated by resorting to the Genetic Algorithm NSGA-II.

Findings – In this paper, the results obtained by means of the optimizations have broadly discussed. The optimal values of the reactances of the compensation networks show a clear trend in the receiving part of the circuit. On the other hand, the problem seems very sensitive to the values of the reactances in the transmitting circuit.

Originality/value – Dynamic wireless power transfer system is one of the newest ways of recharging electric vehicles. Hence, the design of compensation networks for this kind of systems is a new topic, and there is the need to investigate possible solutions to obtain a good performance of the recharging system.

Keywords Finite element analysis, Dynamic wireless power transfer, Compensation networks

Paper type Research paper

COMPEL - The international journal for computation and mathematics in electrical and electronic engineering
Vol. 43 No. 4, 2024
pp. 786-801
Emerald Publishing Limited
0332-1649
DOI 10.1108/COMPEL-10-2023-0549

Introduction

Dynamic wireless power transfer systems (DWPTSs), are object of intensive researches since they are expected to enhance the electric vehicle diffusion (Choi *et al.*, 2015; Bi *et al.*, 2016). The first wireless power transfer systems (WPTSs) were developed as a static recharge station, with the transmitting coil buried in the parking area, and intended to be substitutions of the classical plug-in recharger (Choi *et al.*, 2015; Lukic and Pantic, 2013; J2954_202010 Wireless Power Transfer for Light-Duty Plug-in/Electric Vehicles and Alignment Methodology, 2020). The static recharge, already standardized by Society of Automobile Engineers (J2954_202010 Wireless Power Transfer for Light-Duty Plug-in/Electric Vehicles and Alignment Methodology, 2020), requires a vehicle to stop in an equipped parking area for the time required for battery recharge. Innovative dynamic systems might allow to recharge the batteries while driving and are the current challenges in vehicle recharge systems (Choi *et al.*, 2015; Bi *et al.*, 2016; Tan *et al.*, 2019; Di Capua *et al.*, 2021).

A wireless recharge system, both in static and dynamic solution, comprises a receiving coil mounted on the bottom of the vehicle frame, and one or a set of inductors, the transmitting coils, positioned under the road surface (Choi *et al.*, 2015; Li and Mi, 2015). Wireless power transfer systems make use of magnetic induction to transfer the power from the transmitting coil to the receiving coil (Bi *et al.*, 2016; Feng *et al.*, 2020; Sun *et al.*, 2018). Each coil is equipped with a ferrite layer to concentrate the magnetic flux and to shield the leakage electromagnetic field. The width of the air gap between the coils depends on the vehicle model (J2954_202010 Wireless Power Transfer for Light-Duty Plug-in/Electric Vehicles and Alignment Methodology, 2020).

The power transferred to the load, i.e. the battery, depends on the compensation network connected to both the transmitting and receiving coil (Zhou *et al.*, 2020; Dashora *et al.*, 2018; Chen *et al.*, 2020; Zhang and Mi, 2016). The design of the compensation network aims to increase the power transferred to the load (Ali *et al.*, 2019; Zhang and Mi, 2016) and the transmission efficiency. During static recharge, the receiving and transmitting coils are in a fixed position that must guarantee their good inductive coupling of the coils; this way the design of the compensation network is relatively easy since the mutual inductance between the coils is known and constant. Conversely, in the dynamic recharge, the vehicle runs over a track formed by a strip of transmitting coils (Barmada *et al.*, 2023; Sandrolini *et al.*, 2023). This way, the mutual inductance experiments a variation during the vehicle movement and the compensation networks have to be designed in order to match different alignment conditions.

In this paper, a strip of inductors buried on the road and one receiving coil that shift over the strip are simulated using finite element analysis (FEA) to compute the mutual and self-inductance for different reciprocal positions. The obtained mutual and self- inductances were used in the circuital model of the resonant system to optimize the compensation networks (CNs) that are able to guarantee the best performance in efficiency and power transmission. The considered CNs are formed by three reactive elements arranged in a "T" topology. With a proper selection of their reactances, this layout allows to reproduce the behaviour of most of the CNs considered in the literature (Bertoluzzo *et al.*, 2023). For this reason, these CNs have been considered in the literature (Bertoluzzo *et al.*, 2022a, 2022b, 2022c) devoted to the optimization of a static WPTS. A DWPTS is analysed in a study (Bertoluzzo *et al.*, 2022a, 2022b, 2022c), where the "T" CNs are optimized considering the receiving coil is coupled with only one transmitting coil at a time. The presented paper, instead, considers a DWPTS where the receiving coil is coupled with two transmitting coils at a time, thus representing a much more realistic condition. Moreover, the objective functions (OFs) minimized during the optimization are focused on the average of the efficiency and of the transferred power

over different positions, in an attempt to compensate for the variation of the coupling coefficient between the coupled coils while the vehicle moves over the track.

Forward problem

The layout of the DWPTSs consists of a strip of transmitting coils (TxCs) buried below the road surface to form the track. When a vehicle runs over the track, the receiving coil, denoted as "pickup coil", is coupled step by step with one or more TxCs. This arrangement has been studied by means of FEA. The simulated geometry includes five TxCs and the pickup coil, considered perfectly aligned with the main axis of the track (FLUX (Altair), 2024). The TxCs and the pickup coil are identical and composed of 15 turns with an external diameter of 390 mm (Buja *et al.*, 2015). The distance between the centres of the TxCs is set to 750 mm, and the coil gap is 200 mm. All the coils are equipped with a ferrite layer, a plate with a side of 400 mm and of a thickness of 6 mm with an initial relative magnetic permeability of 3,000. The model used for the FEA is represented in Figure 1(a), whereas Figure 1(b) shows a schematic of the model section with the size of the implemented components.

Given the geometry in Figure 1, FEA solves a time harmonic magnetic field problem using Flux 3D (software released by Altair Engineering [1], Inc. Troy MI, USA (FLUX (Altair), 2024)). The coils are represented as ideal current windings that act as magnetic field sources and are characterized by the absence of discretization (non-meshed coils). The magnetic field produced by the non-meshed coils is evaluated using the Biot–Savart formula (Ferrouillat *et al.*, 2015) in a semi-analytical way. In the air volume, the reduced scalar magnetic potential formulation that takes into account the magnetic field produced by the ideal current paths is applied, while the influence of the ferrite volume is treated by the scalar magnetic potential (Meunier, 2008; Dughiero *et al.*, 2012; Binns *et al.*, 1992; Dughiero *et al.*, 2010):

$$\nabla \cdot \mu_0 \boldsymbol{H}_s = \nabla \cdot \mu_0 \nabla \Phi_R \tag{1}$$

$$\boldsymbol{H} = \boldsymbol{H}_s - \nabla \Phi_R \tag{2}$$

where Φ_R is the scalar magnetic potential and H_s is the magnetic field generated by the coil and computed using the Biot–Savart law.

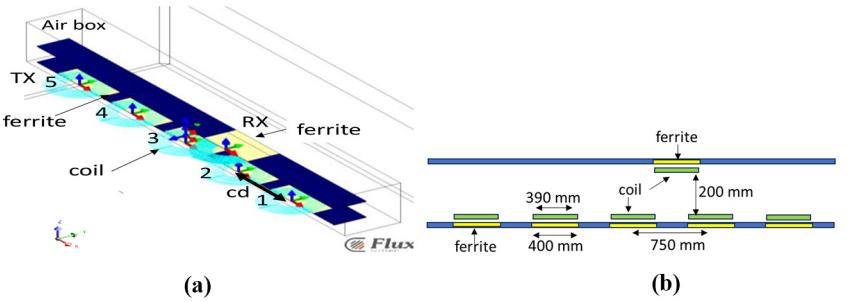

Figure 1.
Layout of the DWPT system model considered for the FEA

Notes: (a) FEA 3D model; (b) schematic of the vertical section with size
Source: Figure created by authors

The ferrite volume is described as a continuous strip. The material of the strip is modified according to the position of the coil, and it is air if the coil is not faced on it and acquires the ferrite properties when a coil is faced on a given position (Dughiero *et al.*, 2012). The typical mesh has 344,000 nodes and 1,975,000 first-order volume elements.

FEA is used to evaluate the lumped parameters of the equivalent circuit representing the recharge system. In particular, the self-inductance of the TxCs and the pickup coil have been assessed, and their mutual inductance for different relative positions like in the literature (Bertoluzzo *et al.*, 2022a, 2022b, 2022c).

To this end, the FEA has been performed by supposing that the pickup coil is supplied with an alternate current having an amplitude of 1 A at the frequency $f_0 = 85$ kHz (Tan *et al.*, 2019). A number of simulations have been performed considering different positions of the pickup coil, starting from Position A of Figure 2, centred over the TxCa, and moving to the right with step of 50 mm up to Position B, centred on the TxCb. In each position, the mutual inductance between the pickup coil and the five TxCs, i.e. coils TxCa, TxCb, TxCc, TxCd and TxCe, have been computed.

From the FEA, it resulted that when the pickup coil is centred on one of the TxCs, its coupling with the two adjacent ones is about 1% of the coupling existing with the aligned coil. For each position of the pickup coil on the strip of TxCs, the self and mutual inductances are computed. In particular, Figure 3 shows the mutual inductance between the pickup coil and the transmitting coils, TxCa and TxCb, respectively, for different positions

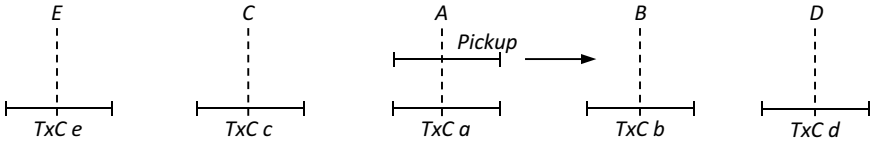

Source: Figure created by authors

Figure 2.
Pickup coil positions considered for the FEA

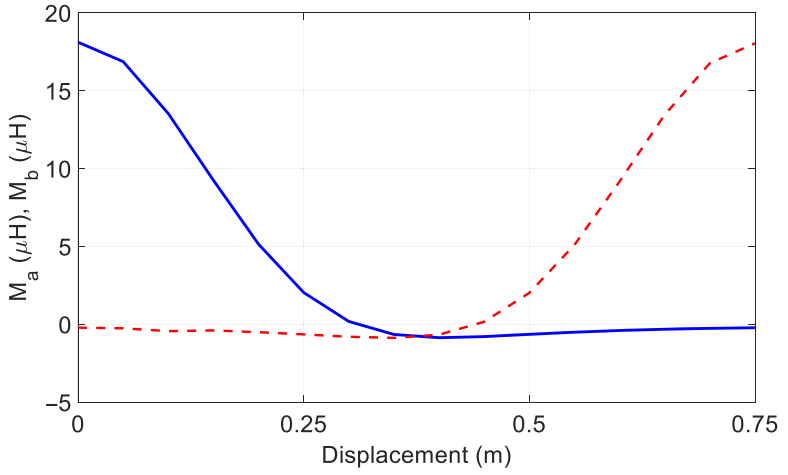

Source: Figure created by authors

Figure 3.
Mutual inductance M_a (solid blue) and M_b (dashed red) obtained by FEA

of the pickup coil. When the pickup coil is aligned to the coil TxCa, the mutual inductance M_a (mutual inductance between TxCa and the pickup coil) is maximum and M_b (mutual inductance between TxCb and the pickup coil) is minimum and vice versa.

For this reason, the model is accurate even if only two TxCs are considered in the simulation. This condition also entails that in a real system, only two coils can be energized at a time, given that there is no advantage in supplying more than two.

Optimization problems

The performance of a DWPT system is greatly influenced by the CNs of the coils. The CNs are formed by reactive elements and operate as interfacing circuits between the power supply generator and the TxCs and between the pickup coil and its equivalent load.

The proposed design considers the pickup coil equipped with three capacitive or inductive elements arranged in a "T" topology and assumes that all the TxCs are connected to equal CNs with "T" topology, each formed by three capacitive or inductive elements. Following from the results of the FEA, the equivalent electrical circuit of the pickup coil and of the TxCs can be represented as in Figure 4.

In the equivalent circuit, only the two TxCs, which the receiving coil is overlapped to, are considered; the mutual coupling with the other coils can be disregarded. The actual load connected to the CN of the pickup coil is constituted by the cascade of a rectifier/battery charger and by the battery. All these elements absorb only active energy so that they can be represented by the equivalent resistance R_L.

To solve the optimization problem, three objective functions (OFs) are formulated as follows:

$$\mathrm{OF1}: P_{Ls}(\mathrm{X}) = \frac{\sum_{i=1}^{\mathrm{Ns}} P_{Li}(X, x_i)}{\mathrm{Ns}} \tag{3}$$

$$\mathrm{OF2}: \eta_{\mathrm{a}}(\mathrm{X}) = \frac{P_{L,\mathrm{TOT}}(X)}{P_g(X)} \tag{4}$$

$$\mathrm{OF3}: P_{\eta}(X) = \sum_{i=1}^{\mathrm{Ns}} P_{Li}(X, x_i) \cdot \eta_i(X, x_i) \tag{5}$$

where P_{Ls} is the average power on the load; P_{Li} is the power on the load at the x_i position with respect to the transmitting coil strip; X is the vector of six unknown reactances;

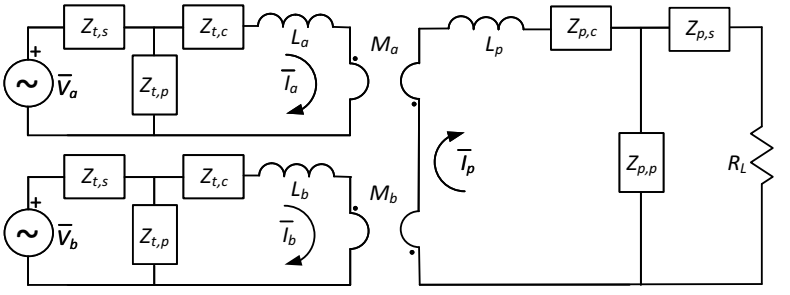

Figure 4.
Equivalent electric circuit of the pickup and of the two coupled TxCs

Source: Figure created by authors

N_s is the number of relative positions of the pickup-TxCs considered in the computation (e.g. in the example $N_s = 16$); η_a is the average efficiency computed as the ratio between the total power supplied to the load, $P_{L,\mathrm{TOT}}$, and the total generated power P_g; P_η is the summation of the products of power and efficiency at each considered position. OF3 is defined on purpose to improve the energetic performance at each position.

Based on the three aforementioned objective functions, two optimization problems have been defined and solved.

Problem (1) Find the values of the reactances X_i with $i = 1,\ldots,6$ of the CNs that simultaneously maximize OF1 and OF2 according to Pareto-like optimality.

Problem (2) Find the values of the reactances X_i with $i = 1,\ldots,6$ of the CNs that simultaneously maximize OF2 and OF3 according to Pareto-like optimality.

The following remarks can be put forward: Problem (1) is focused on the performance of the DWPT system, in terms of transmitted power and efficiency. In Problem (2), OF3 is introduced to avoid solutions with high transmitted power but low efficiency or low transmitted power and high efficiency.

It is worth highlighting that no resonance condition is imposed in any of the Problems. This condition, indeed, should be enforced "automatically" by the optimization process if it results useful for the optimization of the Problems' solutions, as shown in a study (Binns *et al.*, 1992). In the same way, the variation of the resonance frequency with the relative positions of the coils is inherently considered in the optimization process given that the OFs consider the average values of power and efficiency along the vehicle run.

Being the power transfer based on the inductive coupling between the TXCs and the pickup coil, there is no advantage in injecting a direct current component in the TXCs. This component, indeed would not transfer any power to the pickup coil but would cause Joule losses in the TXCs, in their CNs and in the supply inverters. On the other hand, current components at frequencies much higher than the supply frequency should be avoided because they cannot be controlled by the supply inverters and could cause faults in the power switches. For these reasons, the impedance seen at low and high frequency at the inverters output must be as high as possible. To this end, the two additional constraints given by equations (6) and (7):

$$X_{\omega 0.01} > X_\omega \tag{6}$$

$$X_{\omega 100} > X_\omega \tag{7}$$

Equation (6) considers the low-frequency current components and requires that at a frequency equal to 0.01 times the supply frequency ω, the impedance $X_{\omega 0.01}$ seen at the inverter output must be higher that the impedance X_ω seen at the supply frequency. Equation (7) requires that at a frequency equal to 100 times the supply frequency, the impedance $X_{\omega 100}$ seen at the inverter output must be higher that the impedance seen at the supply frequency.

Optimization algorithm

The design variables of the optimization problem are the six reactances, three reactance for the receiving side and three for the transmitting side, since the authors hypothesize the same compensation network for all the coils that form the transmitting strip.

In this paper, the classical NSGA-II algorithm was used to optimize optimization Problems 1–2 (Bertoluzzo *et al.*, 2022a, 2022b, 2022c; Deb *et al.*, 2002). The population size is 50 individuals and NSGA-II run 200 times to find the Pareto front.

For each individual, the OFs are computed numerically by means of a Matlab function that has the six optimized rectances as input and supplies at the output the values of the OFs and of $X_{\omega 0.01}$ and $X_{\omega 0.01}$. In computing its output, the function solves the circuit sketched in Figure 4. The OFs are related to the efficiency and the transferred power in different relative positions of the pickup coil with respect to the TxCs. As a consequence, the circuit is solved for each of these positions, using the corresponding values of the inductive parameters L_a, L_b, M_a and M_b obtained from the model shown in Figure 1. To simplify the computation of the OFs, the coupling between the TxCs is disregarded. Being the coils endowed with ferrite cores, their self-inductance depends on the relative positions and varies from 115.5 μH to 114.4 μH. The maximum mutual inductance between one TxC and the pickup is 18.1 μH. The equivalent series resistance of the coils is supposed to be equal to 0.5 Ω. The supply voltage of the TxCs is sinusoidal with an amplitude of 300 V.

Optimization results

Optimization Problem (1)

In this problem, the optimized quantities are the average transmitted power, equation (1), and the average power transmission efficiency, equation (2), both computed considering different positions of the pickup coil with respect to the TxCs.

The Pareto front obtained by solving the optimization Problem (1) is shown in Figure 5.

Each of the lines reported in Figure 6 represents the actual values of the efficiency vs the transferred power achieved in the different positions of the pickup coil. The circle at the end of each line highlights the transferred power-efficiency condition relevant to Position A (fully aligned position, see Figure 2). When the pickup coil moves toward Position B, the efficiency and, in most cases, the power monotonically decreases to zero. In a few cases, the *locus* of points relating efficiency to power is even a multi-valued one, and the maximum power transferred to the load does not occur when the coils are fully aligned.

The lines relevant to the 50 individuals can be roughly split into two sets by the dashed straight-line in Figure 6. Above this line, the transferred power is nearly maximum in

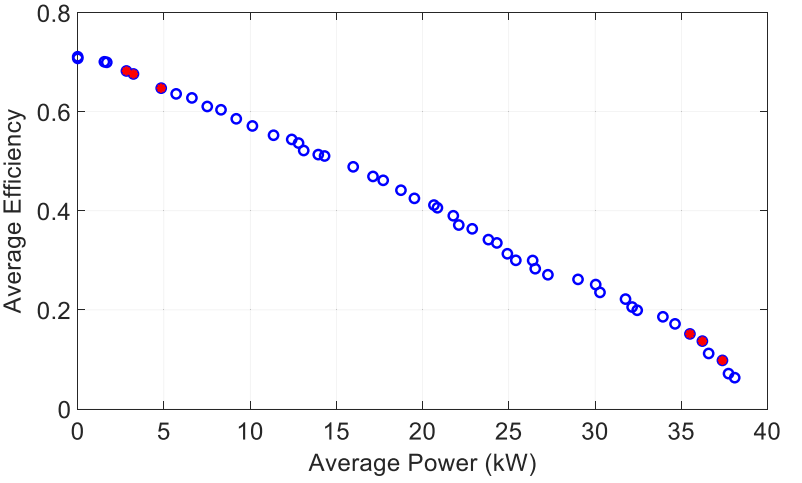

Figure 5.
Pareto front of optimization Problem (1)

Source: Figure created by authors

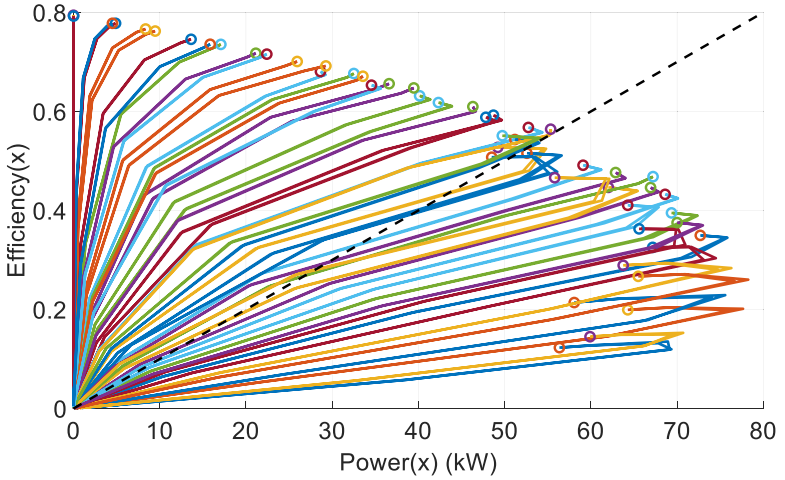

Notes: Each coloured line refers to one point in Figure 5 and is relevant to the trajectory from A (circle, fully aligned coils) to B. The origin of the axes is relevant to the fully misaligned coils
Source: Figure created by authors

Figure 6. Efficiency vs transferred power characteristic of 50 individuals

Position A. Under this line, the transferred power changes in a non-monotonic way from Position A to Position B.

In the following analysis some individuals of each set are considered: three individuals characterized by a transferred power around 10 kW and by a rather high efficiency, highlighted by the red circles in the high-left end of the Pareto front of Figure 5, and the three individuals that transfer the maximum power at the expenses of a lower efficiency, corresponding to the red circles in the low-right end of the front. These two triplets are denoted as the high-efficiency individuals (HEIs) and high-power individuals (HPIs).

The profiles of the transferred power and of the efficiency for the six selected individuals are reported in Figure 7. Figure 7(a) highlights the expected condition by which in the three HPIs the maxima of the transferred power do not coincide with Position A or Position B.

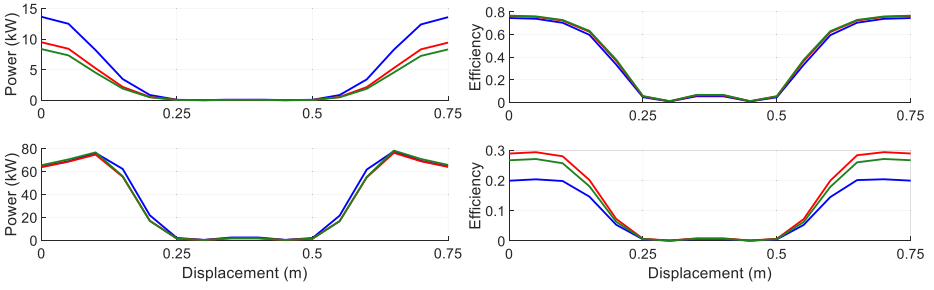

(a) **(b)**

Source: Figure created by authors

Figure 7. (a) Transferred power and (b) efficency of the HEIs (top) and of the HPIs (bottom)

This behaviour is similar to that found when the simple series–series compensation is used and required to reduce the supply voltage of the TxCs whenever the pickup coil approaches them or departs from them to avoid any over-solicitation of the DWPTS components.

The HEIs and the HPIs exhibit a somehow dual performance: the three HEIs have almost the same efficiency [see Figure 7(b), top] in all positions of the pickup coil but they transfer different power [see Figure 7(a), top] while the HPIs transfer the same power [see Figure 7(a), bottom] but with different efficiencies [see Figure 7(b), bottom].

The reactance values of the optimal CNs of the selected HEIs and HPIs are listed in Table 1.

In all the considered individuals, the reactance $X_{t,s}$ of the CN element $Z_{t,s}$, which is connected in series to the supply system, is capacitive, thus assuring that no direct component of current can flow in the circuit.

The reactances $X_{p,s}$, $X_{p,p}$ and $X_{p,c}$ have almost the same values for all the individuals. In particular, it seems that a high inductance is preferred for the $Z_{p,p}$ bipole. Also reactances $X_{t,s}$ and $X_{t,p}$ have similar values, while the values of $X_{t,c}$ vary the most along with the individuals. All in one, this optimization problem seems very sensitive to variables $X_{t,s}$ and $X_{t,p}$ because small variations of these design variables cause a large difference in the behaviour of the system.

The reactances of individuals HEI_1 and HPI_1 have been used in a circuital simulation developed in the Matlab/Simulink environment to check if the performance relevant to power transfer and efficiency, calculated numerically to implement the OFs used for the optimization algorithm, match with those coming from a more realistic model. In the simulations, a vehicle running at 130 km/h has been considered, so that the time taken to move from the Position A to Position B is about 0.021 s.

Figure 8(a) is relevant to HEI_1. It shows the profiles of the total power P_s supplied by the supply generator and the power P_L delivered to the equivalent load while the vehicle moves from Position A to B and then ahead to the next coil. The solid line plots refer to the simulation results while the dashed line plots refer to the values computed numerically. Figure 8(b) shows the power transfer efficiency obtained from the simulation (solid line) and from the numerical computation (dashed line). By inspection of the figure, it appears as the matching between the simulation and the numerical results is good enough to be confident in the performance of the algorithm set up to compute the OFs.

The same quantities have been computed considering HPI_1. They are plotted in Figure 9.

Also in this case the correspondence between the simulation and the analytical results is satisfactory. However, it is clear that a power of 400 kW is not feasible in view of a practical implementation: these HPIs are interesting because of their non-monotonic behaviour in the power-efficiency plane (see Figure 6) during the pickup coil movement.

The same simulations have been carried out again inserting in the model of the system the mutual inductance existing between the two TxCs, which, depending on the position of

	HEI_1	HEI_2	HEI_3	HPI_1	HPI_2	HPI_3
$X_{t,s}$	−8.56	−8.44	−8.76	−7.79	−7.64	−7.53
$X_{t,p}$	12.55	12.72	12.69	9.25	9.20	9.06
$X_{t,c}$	−54.79	−60.33	−61.15	−16.95	−22.72	−22.81
$X_{p,s}$	−106.08	−106.00	−105.51	−107.37	−106.44	−107.12
$X_{p,p}$	370.59	370.66	370.37	372.24	372.21	371.53
$X_{p,c}$	45.92	45.88	45.61	44.70	44.10	44.03

Table 1.
Reactances of the CNs of the TxCx and of the pickup coil

Source: Table created by authors

the pickup coil, ranges from about 0.2 μH to 0.4 μH. The obtained results compared with those coming from the numerical computation are reported in Figures 10 and 11. The first of them, relevant to HEI_1, demonstrates that the simulation results are nearly equal to those obtained by neglecting the TxCs mutual coupling, so that it can be concluded that the optimized CNs are robust against its variation. In the case of HPI_1, considered in Figure 11, the sensitivity of the CNs to the mutual coupling results a little higher, especially when the pickup coil is not aligned with the TxCs, and this causes an increasing of the supply power and a consequent decreasing of the efficiency. In any case, the results of the simulations are comparable with those coming from the numerical computation.

Optimization Problem (2)

In this problem, the optimized quantities are the average product of the transmitted power by the relevant efficiency (3), and the average power transmission efficiency (2), both computed on the different positions of the pickup coil with respect to the TxCs.

The Pareto front obtained by the solution of the optimization Problem (2) is shown in Figure 12.

The efficiency as a function of the transferred power in different positions of the pickup coil is represented in Figure 13. Also in this case, 50 individuals are considered, each line of Figure 13 pertaining to one of them.

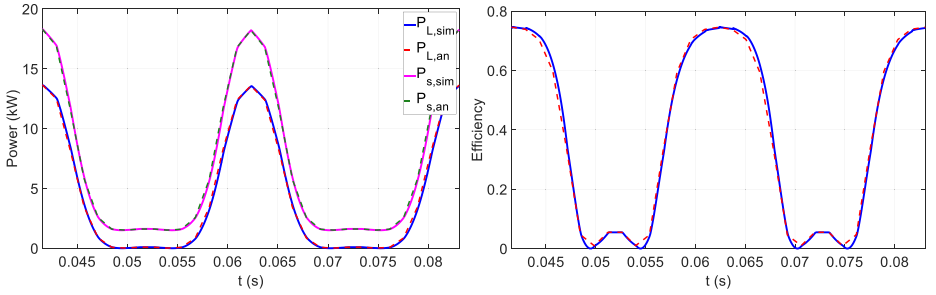

Source: Figure created by authors

Figure 8.
(a) Supplied and transferred power and (b) power transfer efficiency obtained from simulation (blue solid line) and from the objective function (dashed red line)

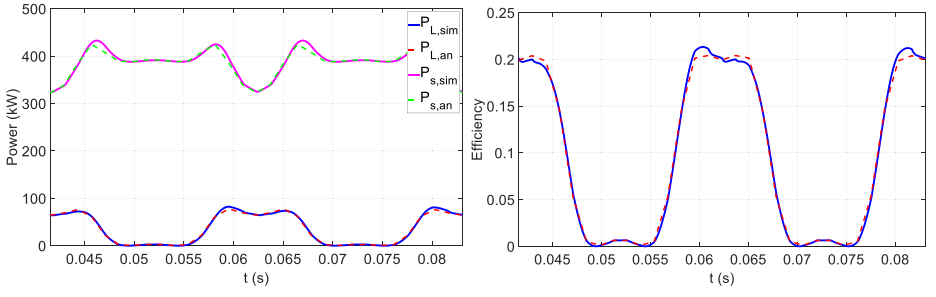

Source: Figure created by authors

Figure 9.
(a) Supplied and transferred power and (b) supplied and transferred power (simulation considers mutual coupling between the TxCs)

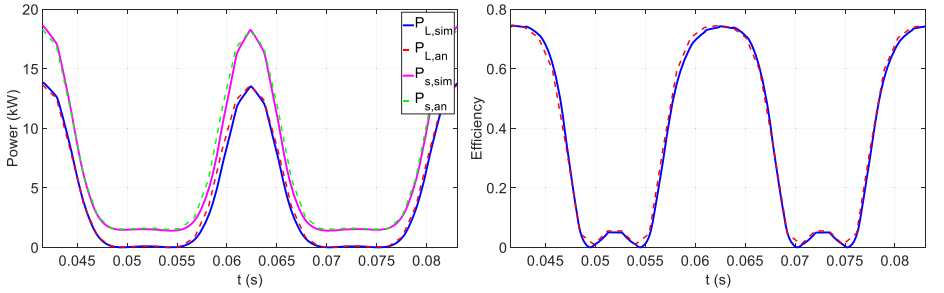

Notes: (a) Supplied and transferred power (simulation considers mutual coupling between the TxCs) and (b) power transfer efficiency obtained from simulation (blue solid line) and from the objective function (dashed red line). Simulation considers mutual coupling between the TxCs
Source: Figure created by authors

Figure 10.
Solutions labelled HEI_1

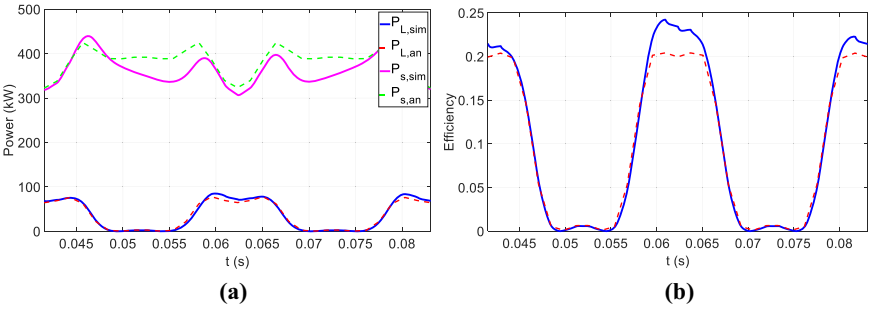

Notes: (a) Supplied and transferred power (simulation considers mutual coupling between the TxCs) and (b) power transfer efficiency obtained from simulation (blue solid line) and from the objective function (dashed red line). Simulation considers mutual coupling between the TxCs)
Source: Figure created by authors

Figure 11.
Solutions labelled HPI_1

The figure shows that in most of the individuals, a comparatively high efficiency is maintained in a rather large power interval while only the few individuals, whose power-efficiency characteristics fall on the left of the dashed line, exhibit an efficiency constantly increasing with the transferred power.

In the following analysis, two triplets of individuals have been selected. The first set is characterized by an efficiency higher than 70% but their transferred power is lower than 1 kW. It is highlighted by the red circles in the left-upper end of the Pareto front in Figure 12 and is denoted as the HEIs set. The other set has a lower but higher than 65% efficiency, and it allows to transfer a much higher power that reaches 7.5 kW. These three individuals are positioned roughly on the first quarter of the Pareto front and are denoted as the HPIs.

The profiles of the transferred power and of the efficiency for the six selected individuals are reported in Figure 14.

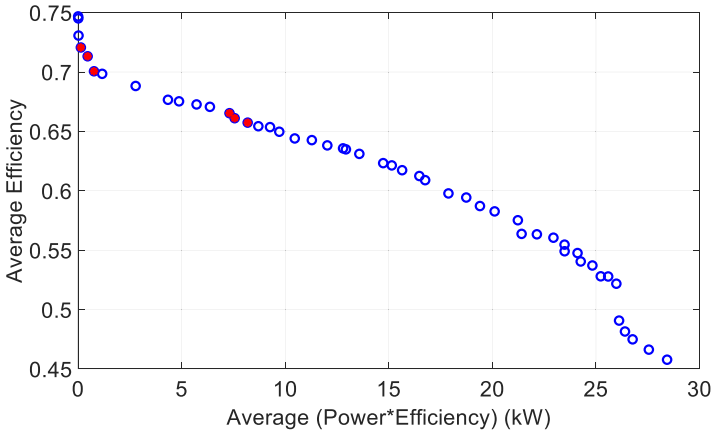

Source: Figure created by authors

Figure 12.
Pareto front of optimization Problem (2)

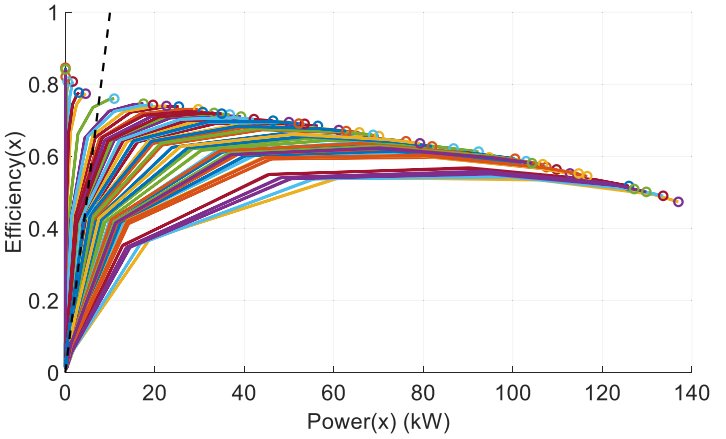

Notes: Each coloured line refers to one point in Figure 12 and is relevant to the trajectory from A (circle, fully aligned coils) to B. The origin of the axes is relevant to the fully misaligned coils

Source: Figure created by authors

Figure 13.
Efficiency vs transferred power characteristic of 50 individuals

Differently from the results coming from Problem (1), now all the individuals reach the maximum transferred power in Position A or in Position B, where the pickup coil is aligned with one of the TxCs, whilst in some individuals the maximum efficiency is reached out of these positions.

The optimal reactances that form the CNs are listed in Table 2. The CNs of the three HPIs are quite similar, while those relevant to the HEIs have some differences. For both sets of individuals, the reactance $X_{t,c}$, connected in series to the TxC compensates for the self-inductance of the coils itself, thus implementing a series compensation.

Simulations have been carried out to check the correspondence between the results coming from the numerical computation of the OFs and those obtained from a more detailed model of the system that also encompasses the effect of the mutual coupling between the TxCs. As an example, the power profiles and the efficiency obtained from the individual HPI_1 are reported in Figure 15.

In both cases, there is a good correspondence between the simulation and the analytical results that confirms also in this case the low sensitivity of the CNs to the mutual coupling between the TxCs.

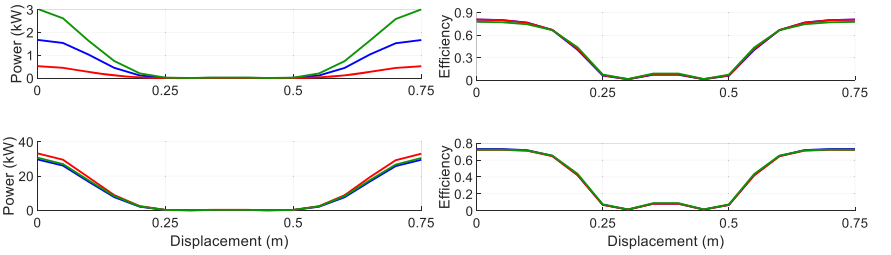

Figure 14.
(a) Transferred power of the HEIs (top) and of the HPIs (bottom) and (b) efficiency of the HEIs (top) and of the HPIs (bottom)

Source: Figure created by authors

	HEI_1	HEI_2	HEI_3	HPI_1	HPI_2	HPI_3
$X_{t,s}$	−15.35	−32.76	−14.44	−4.24	−3.85	−4.26
$X_{t,p}$	119.66	136.72	15.24	4.64	4.24	4.35
$X_{t,c}$	−65.64	−65.85	−67.05	−64.46	−64.68	−64.64
$X_{p,s}$	−89.56	−91.45	−104.86	−104.43	−106.57	−106.57
$X_{p,p}$	325.23	276.44	332.07	330.06	331.68	331.88
$X_{p,c}$	27.13	30.46	48.29	46.52	49.05	50.37

Table 2.
Reactances of the CNs of the TxCx and of the pickup coil

Source: Table created by authors

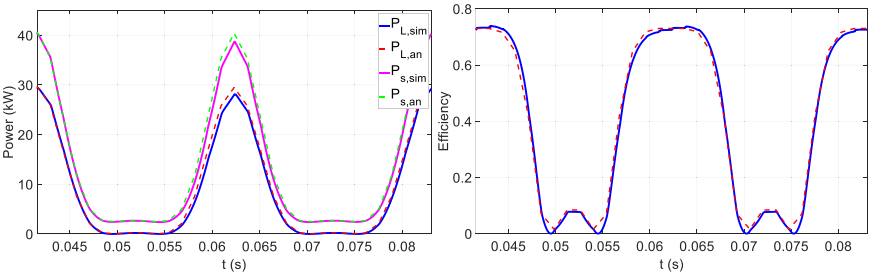

Figure 15.
(a) Supplied and transferred power (simulation considers mutual coupling between the TxCs) and (b) power transfer efficiency obtained from simulation (blue solid line) and from the objective function (dashed red line)

Source: Figure created by authors

Discussion

The analysis of the results obtained by solving the two optimization problems and of the related comments, reported in the previous sections, allows to establish that a DWPTS sized according to the solutions of the optimization Problem (2), which maximizes the product of the transmitted power by the efficiency, is more suitable. Indeed, from Figures 7 and 14, it comes that these individuals originate DWPTSs that exhibit an efficiency from two to three times higher than the efficiency reached by the system sized according to the solutions of the optimization Problem (1). On the other side, the figures show that the power transferred by the DWPTSs coming from the optimization Problem (2) is about half of the power transferred by the other ones. Nevertheless, this is not a serious drawback. Indeed, in conventional battery chargers there is a tendency to increase the transferred power as much as possible, compatibly with the battery's capability, to minimize the charging time. In the case of DWPTSs, however, this last parameter is not so important given that charging occurs while the vehicle is being used. Consequently, the vehicle would have an infinite range and no charging time should be considered if it were possible to transfer onboard the average power used while driving. Considering the average driving power is much lower than the maximum power declared by the vehicle manufacturer, the ability to transfer a power of more than 30 kW when the TXCs and the pickup are aligned can be considered as a good starting point for the sizing of any DWPTS.

It must also be considered that the aim of this paper is to demonstrate the validity of the approach followed for the optimization of a generic DWPTS, without setting any type of specification regarding its performance. When designing a specific DWPTS, the definition of its performance should be the starting point of a recursive process which involves a preliminary design of the system, the selection of the solutions proposed by the optimization algorithm for the CNs, the re-design of the system in accordance with the stresses to which the TXCs and the pickup will be subjected, a new optimization of the CNs and so on until the results converge. This procedure is out of the scope of the paper.

Conclusion

The paper presents the optimization of the CNs of a DWPTS based on an finite element model for mutual inductance calculation. The optimal design of the CNs improves the efficiency and transferred power during the electric vehicle movement. This topic is particularly challenging since the pickup coil experiences maximum and null coupling conditions periodically. The CNs have to be able to improve the power transfer to the battery guaranteeing feasible conditions. The chosen CNs have to preserve efficiency in aligned condition, transfer a reasonable average power and avoid undue solicitations of the coils, the CNs and the supply generator. This paper investigates possible solutions and the most suitable are the ones that improve the efficiency even if they present a power lower than low efficiency solutions. Finally, the power transmitted to the vehicle battery at high efficiency is large enough for effective implementation in the studied device.

Note

1. https://altairhyperworks.com/product/flux

References

Ali, A., Sulaiman, M.I., Yasin, M.N.M., Azizan, M.M., Jusoh, M., Hambali, N.A.M.A. and Mat, M.H. (2019), "Wireless power transfer (WPT) optimization using resonant coil", *Strbske Pleso, Slovak Republic*, p. 20127. doi: 10.1063/1.5118135.

Barmada, S., Musolino, A., Zhu, J. and Yang, S. (2023), "A novel coil architecture for interoperability and tolerance to misalignment in electric vehicle WPT", *IEEE Trans. Magn.*, Vol. 59 No. 5, pp. 1-5, doi: 10.1109/TMAG.2023.3235713.

Bertoluzzo, M., Buja, G., Desideri, D. and Sagar, A. (2023), "A new approach to the analysis of the compensation networks of WPT systems", *IEEE Access*, Vol. 11, pp. 132368-132379, doi: 10.1109/ACCESS.2023.3335170.

Bertoluzzo, M., Di Barba, P., Forzan, M., Mognaschi, M.E. and Sieni, E. (2022a), "Multiobjective optimization of compensation networks for wireless power transfer systems", *COMPEL – The International Journal for Computation and Mathematics in Electrical and Electronic Engineering*, Vol. 41 No. 2, pp. 674-689, doi: 10.1108/COMPEL-06-2021-0204.

Bertoluzzo, M., Di Barba, P., Forzan, M., Mognaschi, M.E. and Sieni, E. (2022b), "Optimization of compensation network for a wireless power transfer system in dynamic conditions: a circuit analysis approach", *Algorithms*, Vol. 15 No. 8, doi: 10.3390/a15080261.

Bertoluzzo, M., Di Barba, P., Forzan, M., Mognaschi, M.E. and Sieni, E. (2022c), "Wireless power transfer system in dynamic conditions: a field-circuit analysis", *Vehicles*, Vol. 4 No. 1, pp. 234-242, doi: 10.3390/vehicles4010015.

Bi, Z., Kan, T., Mi, C.C., Zhang, Y., Zhao, Z. and Keoleian, G.A. (2016), "A review of wireless power transfer for electric vehicles: prospects to enhance sustainable mobility", *Applied Energy*, Vol. 179, pp. 413-425, doi: 10.1016/j.apenergy.2016.07.003.

Binns, K.J., Lawrenson, P.J. and Trowbridge, C.W. (1992), *The Analytical and Numerical Solution of Electric and Magnetic Fields*, Wiley, Chichester.

Buja, G., Bertoluzzo, M. and Mude, K.N. (2015), "Design and experimentation of WPT charger for electric city car", *IEEE Trans. Ind. Electron.*, Vol. 62 No. 12, pp. 7436-7447, doi: 10.1109/TIE.2015.2455524.

Chen, W., Lu, W., Iu, H.H.-C. and Fernando, T. (2020), "Compensation network optimal design based on evolutionary algorithm for inductive power transfer system", *IEEE Transactions on Circuits and Systems I: Regular Papers*, Vol. 67 No. 12, pp. 5664-5674, doi: 10.1109/TCSI.2020.3012700.

Choi, S.Y., Gu, B.W., Jeong, S.Y. and Rim, C.T. (2015), "Advances in wireless power transfer systems for roadway-powered electric vehicles", *IEEE Journal of Emerging and Selected Topics in Power Electronics*, Vol. 3 No. 1, pp. 18-36, doi: 10.1109/JESTPE.2014.2343674.

Dashora, H.K., Buja, G., Bertoluzzo, M., Pinto, R. and Lopresto, V. (2018), "Analysis and design of DD coupler for dynamic wireless charging of electric vehicles", *Journal of Electromagnetic Waves and Applications*, Vol. 32 No. 2, pp. 170-189, doi: 10.1080/09205071.2017.1373036.

Deb, K., Pratap, A., Agarwal, S. and Meyarivan, T. (2002), "A fast and elitist multiobjective genetic algorithm: NSGA-II", *Evolutionary Computation, IEEE Transactions*, Vol. 6 pp. 182-197, doi: 10.1109/4235.996017.

Di Capua, G., Maffucci, A., Stoyka, K., Di Mambro, G., Ventre, S., Cirimele, V., Freschi, F., Villone, F. and Femia, N. (2021), "Analysis of dynamic wireless power transfer systems based on behavioral modeling of mutual inductance", *Sustainability*, Vol. 13 No. 5, p. 2556, doi: 10.3390/su13052556.

Dughiero, F., Forzan, M. and Sieni, E. (2010),"Simple 3D fem models for evaluation of EM exposure produced by welding equipments", *Studies in Applied Electromagnetics and Mechanics, Ios Pr Inc*, pp. 911-919.

Dughiero, F., Forzan, M., Pozza, C. and Sieni, E. (2012), "A translational coupled electromagnetic and thermal innovative model for induction welding of tubes", *IEEE Transactions on Magnetics*, Vol. 48 No. 2, pp. 483-486, doi: 10.1109/TMAG.2011.2174972.

Feng, H., Tavakoli, R., Onar, O.C. and Pantic, Z. (2020), "Advances in high-power wireless charging systems: overview and design considerations", *IEEE Trans. Transp. Electrific.*, Vol. 6 No. 3, pp. 886-919, doi: 10.1109/TTE.2020.3012543.

Ferrouillat, P., Guerin, C., Meunier, G., Ramdane, B., Labie, P. and Dupuy, D. (2015), "Computations of source for non-meshed coils with A–V formulation using edge elements", *IEEE Trans. Magn.*, Vol. 51 No. 3, pp. 1-4, doi: 10.1109/TMAG.2014.2365293.

FLUX (Altair) (2024), available at: https://altairhyperworks.com/product/flux

J2954_202010 Wireless Power Transfer for Light-Duty Plug-in/Electric Vehicles and Alignment Methodology (2020), available at: www.sae.org/standards/content/j2954_202010/

Li, S. and Mi, C.C. (2015), "Wireless power transfer for electric vehicle applications", *IEEE Journal of Emerging and Selected Topics in Power Electronics*, Vol. 3 No. 1, pp. 4-17, doi: 10.1109/JESTPE.2014.2319453.

Lukic, S. and Pantic, Z. (2013), "Cutting the cord: static and dynamic inductive wireless charging of electric vehicles", *IEEE Electrification Mag.*, Vol. 1 No. 1, pp. 57-64, doi: 10.1109/MELE.2013.2273228.

Meunier, G., (Ed.) (2008), *The Finite Element Method for Electromagnetic Modeling*, ISTE; Wiley, London, Hoboken, NJ.

Sandrolini, L., Simonazzi, M., Barmada, S. and Fontana, N. (2023), "Two-port network compact representation of resonator arrays for wireless power transfer with variable receiver position", *International Journal of Circuit Theory and Applications*, Vol. 51 No. 5, pp. 2301-2314, doi: 10.1002/cta.3510.

Sun, L., Ma, D. and Tang, H. (2018), "A review of recent trends in wireless power transfer technology and its applications in electric vehicle wireless charging", *Renewable and Sustainable Energy Reviews*, Vol. 91, pp. 490-503, doi: 10.1016/j.rser.2018.04.016.

Tan, L., Zhang, M., Wang, S., Pan, S., Zhang, Z., Li, J. and Huang, X. (2019), "The design and optimization of a wireless power transfer system allowing random access for multiple loads", *Energies*, Vol. 12 No. 6, p. 1017, doi: 10.3390/en12061017.

Zhang, W. and Mi, C.C. (2016), "Compensation topologies of high-power wireless power transfer systems", *IEEE Transactions on Vehicular Technology*, Vol. 65 No. 6, pp. 4768-4778, doi: 10.1109/TVT.2015.2454292.

Zhou, Z., Zhang, L., Liu, Z., Chen, Q., Long, R. and Su, H. (2020), "Model predictive control for the receiving-side DC–DC converter of dynamic wireless power transfer", *IEEE Trans. Power Electron.*, Vol. 35 No. 9, pp. 8985-8997, doi: 10.1109/TPEL.2020.2969996.

Further readiing

Bavastro, D., Canova, A., Cirimele, V., Freschi, F., Giaccone, L., Guglielmi, P. and Repetto, M. (2014), "Design of wireless power transmission for a charge while driving system", *IEEE Transactions on Magnetics*, Vol. 50 No. 2, pp. 965-968, doi: 10.1109/TMAG.2013.2283339.

Di Capua, G., Femia, N., Stoyka, K., Di Mambro, G., Maffucci, A., Ventre, S. and Villone, F. (2021), "Mutual inductance behavioral modeling for wireless power transfer system coils", *IEEE Trans. Ind. Electron.*, Vol. 68 No. 3, pp. 2196-2206, doi: 10.1109/TIE.2019.2962432.

Suh, I. and Kim, J. (2013), "Electric vehicle on-road dynamic charging system with wireless power transfer technology", 2013 International Electric Machines and Drives Conference, pp. 234-240, doi: 10.1109/IEMDC.2013.6556258.

Corresponding author

Elisabetta Sieni can be contacted at: elisabetta.sieni@uninsubria.it